Characterization and Modeling of Metal-Insulator Transition (MIT) Based Tunnel Junctions

E. Freeman[1], A. Kar[1], N. Shukla[1], R. Misra[1], R. Engel-Herbert[1], D. Schlom[2], V. Gopalan[1], K. Rabe[3], and S.Datta[1]
[1]Pennsylvania State University, PA-16802; [2]Cornell University, NY; [3]Rutgers University, NJ
Phone: (814) 954 2391, Fax: (814) 865 7065, e-mail: exf181@psu.edu

Continued physical scaling will reduce power dissipation primarily through the reduction in device capacitance; however, a far greater benefit would result if the CMOS FET could be replaced by a fundamentally new device scheme that operates under very low supply voltages. Recently, semiconductor based inter-band tunnel field effect transistors (TFET) have been explored due to their potential to achieve sub k_BT/q steep switching swings, enabling low voltage operation [1]. In this work, we explore the abrupt metal to insulator transition (MIT) of vanadium dioxide (VO_2) based tunnel junction – a first step towards a correlated electron based steep switching TFET. As illustrated in Fig.1 the metal insulator transition MIT in materials with strong electron correlation can be utilized to modulate the tunnelling current by opening an energy gap around the Fermi level in the OFF-state, and a metal-insulator-metal tunnelling current by collapsing the gap in the ON-state.

Characterization of VO_2 Based MIT Tunnel Junctions:

Thermally and electrically induced MIT of ultrathin VO_2 films is shown in Fig.2. VO_2 films of 3.8 nm thickness were grown by MBE on TiO_2(001) substrate. The MIT transition temperature shifted to lower values (T_{MIT}=300K) due to residual strain in the film. Two samples were fabricated: one with the the HfO_2 tunel barrier and one without it. The band diagrams for the fabricated devices are illustrated in Fig.3, where a Mott-Hubbard gap of 0.6 eV is expected to exist in the OFF-state [2]. The contact resistivity is extracted from CTLM pads, schematically shown in Fig.4. For VO_2 in the metallic state the contact resistivity ρ_{tunnel}=2.2x10^{-4} Ω-cm^2 (R_{tunnel} = 11 Ω) and ρ_{tunnel}=3.1x10^{-5} Ω-cm^2 (R_{tunnel} = 2.8 Ω) is extracted for devices with 1.6 nm ALD grown HfO_2 and no insulating barrier, respectively (Fig.5). Driving the device thermally across the MIT, the contact resistivities ρ_{tunnel} changed to 2.6x10^{-3} Ω-cm^2 (R_{tunnel} = 1097 Ω) and 7.63x10^{-3} Ω-cm^2 (R_{tunnel} = 850 Ω) with and without tunnel barrier, respectively. These order of magnitude changes in the electron transfer characteristics demonstrate the feasibility to realize tunnel junctions based on correlated electron materials. This corresponds to an on state tunnel conductance ratio of 3.55 taking into account differences in VO_2 sheet resistance. Fig.6 illustrates the simulated J-V curves of a Pd/HfO_2/VO_2 stack assuming metal-insulator-metal and metal-insulator-semiconductor structures for the ON and OFF states, respectively. Reasonable agreement with the experimental data is achieved.

Determination of Underlying Switching Mechanism in VO_2 Based MIT Tunnel Junctions:

The underlying physical origin of the coupled first order phase transition in VO_2 is still debated and is believed to be either a charge induced phase transition (Mott-Hubbard) or structurally driven (Peierls transition). Time dependent characteristics of the electric field induced MIT of VO_2/TiO_2 devices was studied to separate electric field driven (Mott-Hubbard) from temperature induced structural (Peierls) effects. The transient response (1 kHz) of the device is shown in Fig.7a. Further, frequency dependent switching experiments reveal that the MIT is irreversible at or beyond 20 kHz for the same applied voltage, and the MIT device doesn't reversibly switch off (Fig.7b). A delay time of 80-110 µs is observed in Fig.7a before the device transitions, albeit with considerable jitter. The current flow through the resistor is 2 mA and the volume of the device is 1.33x10^{-11} cm^3, therefore the number of carriers injected is approximately 7.5x10^{22}-9.4x10^{22} cm^{-3} as plotted in Fig.8. The carrier density needed to drive the semiconducting VO_2 into the metallic state is given by the Mott criterion $n_c \approx (0.25/\alpha_H)^3$ and $\alpha_H = \hbar^2\varepsilon / m^* q^2$ where $\hbar$ is the reduced Plancks constant, ε is the permittivity of VO_2 in the insulating state (ε ~40) and m* the electron effective mass (~4m_e) resulting in a critical carrier density n_c of 2.1x10^{23} cm^{-3} close to the value extracted from the measurement. Fig.8 shows a rise time (T_{Rise}) of 192 ns; this rise time is limited by the RC in the system and is not the intrinsic transition time of the MIT process in VO_2.

To further investigate the effect of joule heating we employed a 3D multiphysics finite element simulator (COMSOL) to perform heat transfer simulations using the actual device geometry. The increase in the steady state device temperature needed for switching was simulated for various heat pulse widths. The experimentally determined transition voltage and current of 15.21 V and 2.1 mA (OFF state) was used to estimate dissipated power density, yielding Q~4.9x10^{14} W/m^3. Other constants for VO_2 used were density (4340 kg/m^3), specific heat capacity (690 J/K-kg), heat transfer coefficient (20 W/K-m^2) and thermal conductivity (6 W/K-m). The model is beyond a simple one-dimensional heat transfer model [3] and further takes heat dissipation into the contact and substrate into account. The equations and boundary conditions used are given in Table I. Fig.10 shows the simulated temperature distribution in an 8µm experimental device for various supply voltage pulse widths. In Fig.11 the simulated temperature-change (ΔT) in the VO_2 film of the 8µm experimental device is plotted as a function of pulse widths applied. It can be seen that the steady state ΔT achieved for the heat supplied is only 2.98K for a pulse width of 600 µs and ΔT saturates at ~2.9K for all pulse widths > 200 µs. It is also shown in Fig.11 that for an applied pulse width which equals to the field induced OFF to ON state switching time (T_{Rise}=192 ns), the ΔT is only 0.10K. Additionally, the steady state temperature change of ΔT=2.98K for longer pulse width durations is insufficient to cause a phase transition thermally. This suggests that the predominant switching mechanism in the MIT tunnel junction is likely due to charge filling of the conduction band and that Joule heating plays a negligible role in this transition.

[1] Khatami Y. *et al*,. IEEE Trans. Electron Devices, 56 (2009) 11. [2] Berglund, C. N. et. al. Phys. Rev. 185 (1969) 1022.
[3] Stefanovich G. *et. al.*, J. Phys.: Condens. Matter 12 (2000) 8837.

Conductance Modulation in MIT Tunnel Junction

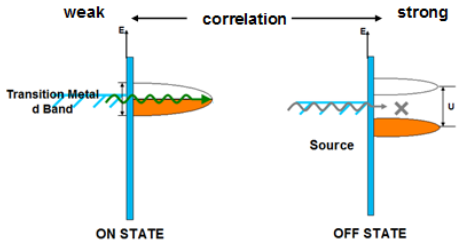

Fig. 1: Schematic band diagram of MIT material controlling tunneling in ON (metallic) and OFF (insulating) state.

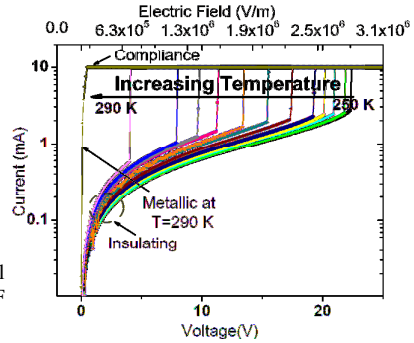

Fig. 2: Thermal and field induced transitions observed.

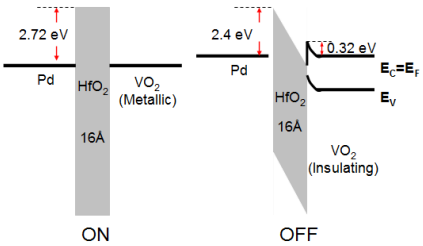

Fig. 3: Equilibrium energy band diagram of Pd/HfO_2/VO_2, in ON-state and OFF-state.

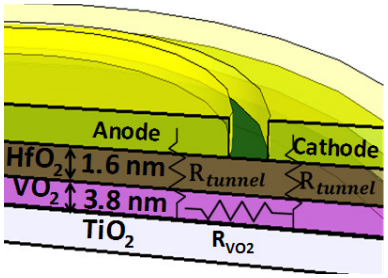

Fig. 4: 3D cross section of the tunneling structure. R_{Tunnel} refers to tunneling resistivity and R_{VO2} is the VO_2 sheet resistance.

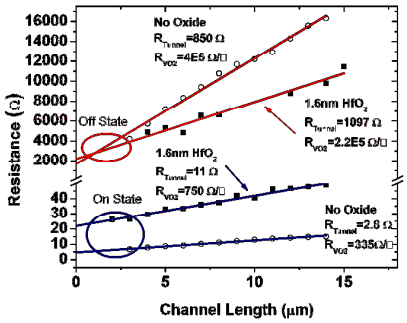

Fig. 5: CTLM data showing a change in contact resistance due to the presence of HfO_2 tunnel barrier.

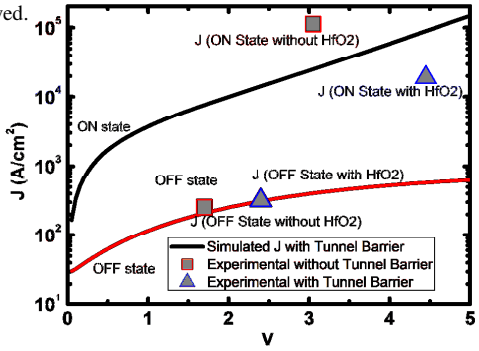

Fig. 6: Simulated current voltage characteristic and experimental conductance ratio in the ON and OFF state.

Switching Mechanism in VO_2: Electric Field Driven vs. Thermally Induced MIT.

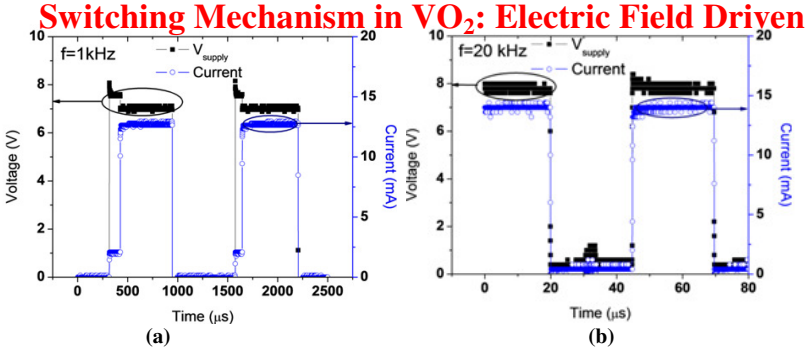

Fig. 7: Frequency dependent switching (FDS) at 275K analysis of non-tunneling device for (a) 1 kHz (b) 20 kHz. Device does not turn OFF beyond 20 kHz.

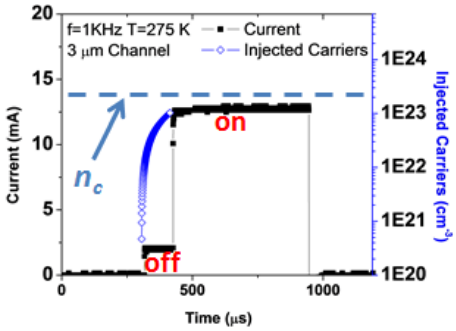

Fig. 8: Injected carrier density in ON state at f=1 kHz is close to Mott carrier density n_c=2.1x10^{23}/cm^3 indicating **field induced transition**.

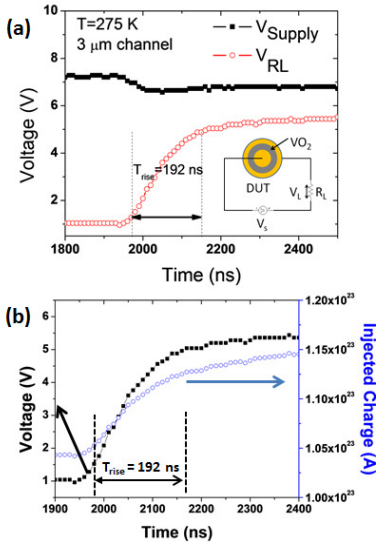

Fig. 9: (a) MIT transition time after the critical density has been achieved is 192 ns, for an R_L of 500 Ω. (b) At the start of the transition ~1x10^{23} carriers are injected, close to the critical Mott carrier density of 2.1x10^{23}/cm^3.

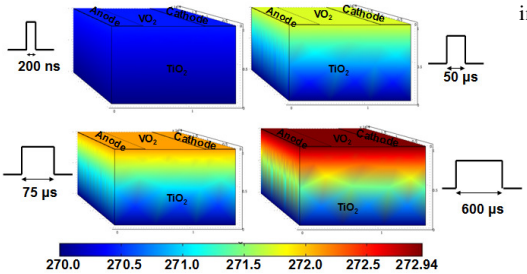

Fig. 10: 3D device simulation of temperature rise for various heat pulse widths applied indicate insufficient Joule heating to cause switching.

Thermal Conduction Model:	$\delta_{Ts}\rho C_p \frac{\partial T}{\partial t} - \nabla(K\nabla T) = Q$
Air/interface boundary conditions using convective heat transfer:	$n.(K\nabla T) = h(T - T_O)$
VO_2/TiO_2 & VO_2/Electrode boundary condition:	$n.(K_1\nabla T_1 - K_2\nabla T_2) = h(T_O - T)$

Table I: Heat balancing equations used for COMSOL.

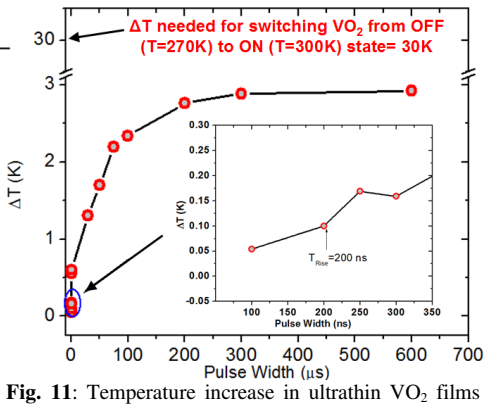

Fig. 11: Temperature increase in ultrathin VO_2 films during FDS measurements. The max temperature increase is one order of magntiude smaller than needed to thermally trigger the phase transition.